*Geopersia* ***5*** *(2), 2015, PP. 177-187*

# The Prediction of the Tensile Strength of Sandstones from their petrographical properties using regression analysis and artificial neural network

**Mohammad Hossein Ghobadi[1]*, Sajeddin Mousavi[2], Mojtaba Heidari[1], Behrouz Rafie[1]**
[1] *Geology Department, Faculty of Science, Bu-Ali Sina University, Hamedan, Iran*
[2] *Geology Department, Faculty of Earth Sciences, Shahid Chamran University, Ahvaz, Iran*
**Corresponding author, e-mail: amirghobadi@yahoo.com*
(*received: 22/11/2014 ; accepted: 25/11/2015*)

**Abstract**

This study investigates the correlations among the tensile strength, mineral composition, and textural features of twenty-nine sandstones from Kouzestan province. The regression analyses as well as artificial neural network (ANN) are also applied to evaluate the correlations. The results of simple regression analyses show no correlation between mineralogical features and tensile strength. However, the tensile strength of the sandstone was decreased by cement content reduction. Among the textural features, the packing proximity, packing density, and floating contact as well as sutured contact are the most effective indices. Meanwhile, the stepwise regression analyses reveal that the tensile strength of the sandstones strongly depends on packing density, sutured contact, and cement content. However, in artificial neural network, the key petrographical parameters influencing the tensile strength of the sandstones are packing proximity, packing density, sutured contact and floating contact, concave-convex contact, grain contact percentage, and cement content. Also, the R-square obtained ANN is higher than that observed for the stepwise regression analyses. Based on the results, ANN were more precise than the conventional statistical approaches for predicting the tensile strength of these sandstones from their petrographical characteristics.

**Keywords:** *Artificial Neural Network, Petrographical Features, Regression Analysis, Sandstone, Tensile Strength.*

## Introduction

Tensile strength ($\sigma_t$) of rocks is one of their most important mechanical properties. This parameter has a crucial role in the design and construction of geotechnical projects such as underground opening, dam foundation, slope stability, as well as rock drillability in tunneling and oil wells (Nova & Zaninetti, 1990; Canakci & Pala, 2007; Gurocak *et al.*, 2012). Moreover, tensile strength of rocks can be governed by many factors such as mineral composition, density, porosity, fabric, moisture content, state of alteration or changes due to weathering, etc. (Prikryl, 2001). This mechanical property is measured experimentally by way of either direct or indirect methods (ISRM, 1981). High-quality core samples of regular geometry are required for the application of tensile strength test in laboratory. However, it is sometimes impossible to obtain such specimens. Under such conditions, a predictive model can be used to determine the strength from other tests such as physical properties, point load strength, and so on.

Likewise, some researchers have undertaken empirical correlations to estimate $\sigma_t$ values in terms of petrographical properties of rocks. Relationships among mineralogical composition, textural properties, and tensile strength of different granitic rocks have been investigated by Merriam et al. (1970). Furthermore, the textural characterization of rocks is related to their mechanical performance, drill ability, and mechanical features such as Brazilian tensile strength (Ersoy & Waller, 1995). The study indicates that a meaningful correlation exists between texture coefficient (TC) and tensile strength. Meanwhile, the petrographical and geomechanical properties of some sandstones from the Newspaper Member of the Natal Group near Durban, South Africa have been evaluated by Bell and Lindsay (1999).They have revealed that the various petrological properties have little or no influence on the mechanical properties or behavior of these sandstones. However, the study showed that as the mean grain size of the sandstones increase, the tensile strength decreases.

On the other hand, the influence of mineral composition and texture on the tensile strength of rocks has been indicated by Tugrul and Zarif (1999). Also, the effect of micro-scale parameters on the macro-scale behavior of sandstone samples tested under Brazilian test conditions has been investigated by Tavallali and Vervoort (2010). The results show that the tensile strength and tensile

fracture pattern of the sandstones are controlled by their grain size and mineral composition. But the grain size effect on these features is more dominant than the effect of mineral content. In addition to these, empirical equations for the prediction of the tensile strength of limestone and marble from microscopic data including their mineralogical properties have been proposed by Ozcelik *et al.* (2012). They have tested the validity of model equations by using multivariate statistical methods.

However, although many predictive models for tensile strength have been proposed for different rocks, relatively little attention has been directed towards developing the models for sandstones. Also, these models are mostly restricted to a few petrographical properties for restricted rock types. Thus, if relationships are achieved, they are not available for sandstones obtained from various locations. For this reason, namely, using sandstone samples acquired from a formation with a given age and depositional environment, the empirical relationships have been reliable. In this study, in order to obtain the relationships between petrographical properties and tensile strength, many sandstone samples of the Aghajari Formation have been brought under study. To this aim, the petrographical characteristics and physical properties as well as tensile strength of these sandstones were determined. Eventually, using statistical methods and artificial neural network (ANN), the empirical equations considering several petrographical indices have been obtained.

## Geology and Sampling

The study area is located in the Zagros zone in southwestern Iran. It lies between longitudes 47° 41' to 50° 39' E and latitudes 29° 58' to 33° 04' N and forms a part of the simply-folded Zagros zone (Fig. 1a); a simply-folded zone consisting of long, linear, and asymmetrical folds. Fold axes have a northwest to southeast trend. Sandstone samples from the Aghajari Formation were selected as the study materials. The formation is a wide outcrop in the southern and southwestern parts of Iran. The Aghajari Formation includes varieties of medium- to coarse-grained, brown-to-grey sandstones, laminated to massive, red marls and siltstones. It belongs to upper Miocene-Pliocene (James & Wynd, 1965). Meanwhile, these sandstones were deposited under fluvial sedimentary environment.

A total of 29 sandstones, obtained from the formation, were sampled from around Khouzestan province at various outcrops (Fig. 1b). In the present study, the specimens were cored in laboratory from fresh sandstone blocks excavated from various outcrops.

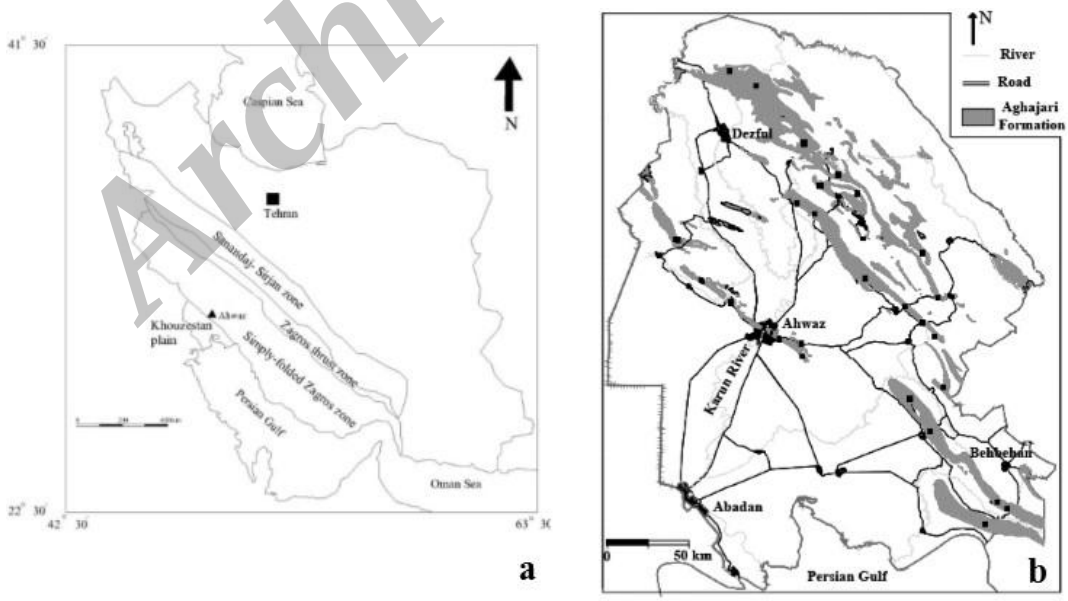


Figure 1. Location and geological maps of study area. (a**)** Location map (b) Distribution of the Aghjari Formation and sandstone sampling sites (■).

Moreover, thin sections of each sandstone block were prepared in order for their mineral and textural features to be examined.

## Materials and Methods

Petrographic properties could only be observed or measured in thin sections. For this reason, petrographical indices characterizing composition and texture of each of the sandstone samples were determined by counting and measuring grains in each thin section under the polarizing microscope (Fig. 2a and 2d). The relative abundance of mineral components was determined by counting 50 randomly selected points in each thin section (Table 1). In order to study textural properties, the thin sections were photographed with a high-resolution camera connected to the polarizing microscope. Photomicrographs were transferred directly and processed on a PC using the AutoCAD 2013 software. In the first step, photomicrographs were digitized in the software for image analysis (Fig. 2c and 2f).

Table 1. Mineral composition of sandstones of the Aghajari Formation

| Sample No. | Rock fragments or Lithics | | | | Q | CH | Fel | Mic | Gyp | Op | Cm |
|---|---|---|---|---|---|---|---|---|---|---|---|
| | CRF | VRF | MRF | SRF | | | | | | | |
| | (%) | | | | | | | | | | |
| 1 | 55 | - | 1 | - | 13 | 6 | 9 | - | - | 5 | 11 |
| 2 | 70 | - | - | - | 2 | 10 | - | - | - | 4 | 13 |
| 3 | 52 | 16 | 3 | - | 8 | 7 | 2 | 1 | - | 5 | 6 |
| 4 | 71 | 13 | - | - | 2 | 3 | 1 | - | - | 5 | 5 |
| 5 | 35 | 18 | 17 | - | 16 | 5 | 5 | 1 | - | 1 | 3 |
| 6 | 70 | 10 | | - | 5 | 9 | 1 | - | 1 | 2 | 1 |
| 7 | 62 | 20 | | - | 5 | 2 | 2 | - | - | 8 | 1 |
| 8 | 28 | 33 | 14 | - | 14 | 2 | 3 | - | - | 7 | - |
| 9 | 52 | 10 | 8 | - | 15 | 3 | 5 | - | - | 6 | - |
| 10 | 76 | 3 | | 4 | 5 | 1 | 1 | - | - | 10 | - |
| 11 | 61 | 12 | 12 | - | 7 | 1 | 2 | - | - | 5 | - |
| 12 | 51 | 7 | 8 | - | 20 | 3 | 5 | 1 | - | 5 | - |
| 13 | 64 | 4 | - | - | 6 | - | - | - | - | 6 | 23 |
| 14 | 54 | 15 | 1 | 1 | 10 | 3 | 2 | - | - | 4 | 10 |
| 15 | 45 | 15 | 1 | 2 | 18 | 4 | 1 | - | - | 2 | 11 |
| 16 | 56 | 15 | - | 2 | 10 | 7 | 1 | - | - | 3 | 6 |
| 17 | 63 | 12 | 2 | - | 10 | - | 1 | - | - | 5 | 7 |
| 18 | 50 | 9 | 1 | 9 | 11 | 10 | 7 | - | - | 9 | 1 |
| 19 | 60 | 4 | 1 | 8 | 5 | 10 | - | - | - | 5 | 1 |
| 20 | 70 | 3 | - | 2 | 3 | 4 | - | - | - | 3 | 15 |
| 21 | 63 | 4 | 1 | 3 | 15 | 4 | 2 | - | - | 4 | 5 |
| 22 | 70 | 3 | 1 | 1 | 10 | 2 | 3 | - | - | 3 | 7 |
| 23 | 47 | 8 | 3 | - | 15 | 4 | 2 | 1 | - | 2 | 18 |
| 24 | 55 | 11 | 1 | - | 13 | 5 | 4 | - | - | 2 | 9 |
| 25 | 58 | 1 | 15 | - | 10 | 1 | 4 | 1 | - | 5 | 5 |
| 26 | 34 | 15 | 3 | - | 18 | 5 | 3 | - | - | 4 | 18 |
| 27 | 40 | 15 | 3 | - | 15 | 4 | 3 | - | - | 5 | 16 |
| 28 | 63 | 2 | 2 | - | 9 | 4 | 3 | - | - | 7 | 10 |
| 29 | 53 | 6 | 5 | - | 10 | 3 | 1 | - | - | 5 | 17 |
| Mean | 55.93 | - | - | 1.1 | 10.34 | 4.21 | 2.52 | 0.17 | - | 4.72 | 7.55 |
| SD | 11.87 | - | - | 2.3 | 5.01 | 2.88 | 2.15 | 0.38 | - | 2.12 | 6.7 |

CRF: Carbonaceous rock fragments, VRF: Volcanic rock fragments, MRF: Metamorphic rock fragments, SRF: Muddy rock fragments, Q: Quartz, CH: Chert, Fel: Feldespars, Mic: Mica, Gyp: Gypsum, Op: Opaque minerals, Cm: Cement, SD: Standard deviation

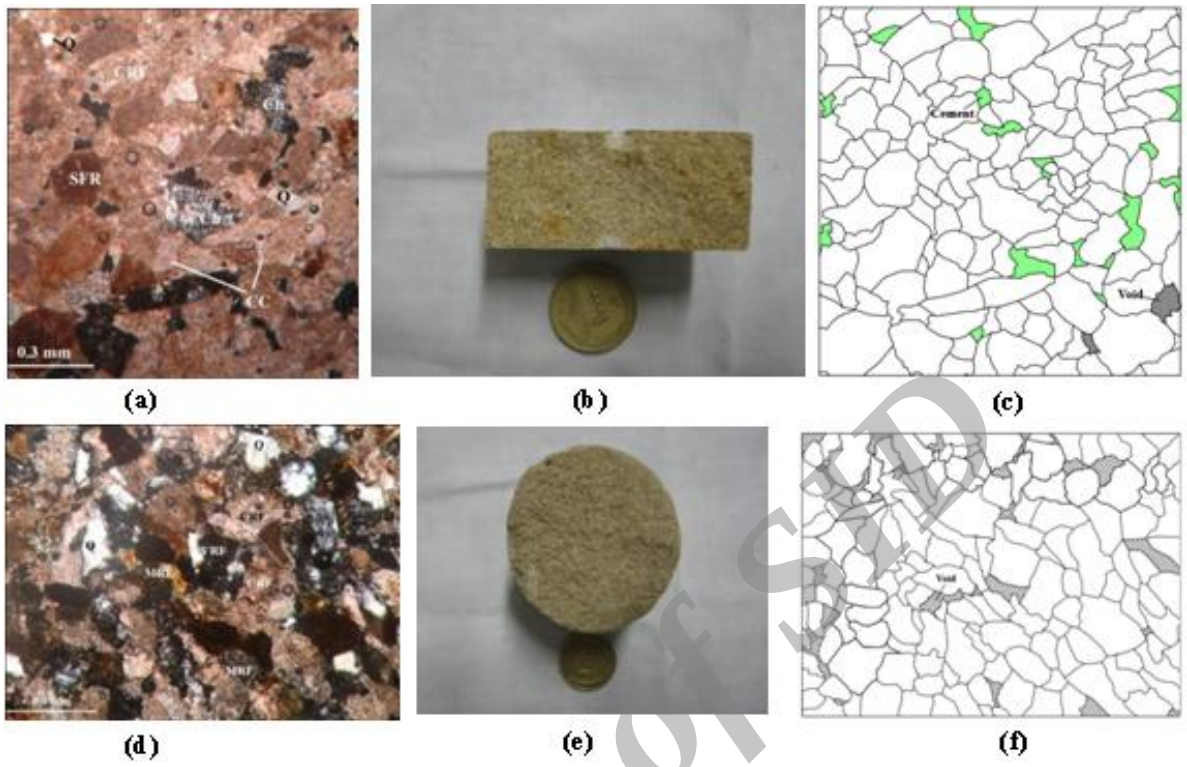


Figure 2. The typical petrographic images of the studied sandstones. (a) Photomicrograph of sandstone no. 2 (b) Grab sample of sandstone no. 2 (c) Digitizing photomicrograph of sandstone no. 11 (d) Photomicrograph of sandstone no. 11 (e) Grab sample of sandstone No. 11 (f) Digitizing photomicrograph of sandstone No. 11 (Q: quartz, CRF: carbonaceous rock fragment, VRF: Volcanic rock fragment, MRF: muddy rock fragment, Ch: chert, CC: calcit cement)

Using the digitized images, then, textural features were quantified. Accordingly, grain shape and size are characterized by the grain's length (L), width (W), area (A), and perimeter (P). Five random fields of view per thin section were evaluated for this purpose. These features are used to formulate several coefficients such as aspect ratio (AR=L/W) and form factor ($FF=4\pi A/P^2$). The arrangement of particles in a sandstone involves the concept of packing, which can be assessed in terms of packing proximity (measure of the spacing between grains) and packing density (measure of grain packing arrangements) as proposed by Kahn (1956). These parameters were measured along five traverse lines per thin section (Table 2). On the other hand, the types of grain-to-grain contacts and their percentages were determined. Grain contact (GC) is the ratio of the grain's total length to the length of contact a grain has with its neighbors (Dobereiner & De Freitas, 1986). The index was appraised using 100 randomly selected grains. Meanwhile, grain area ratio (GAR) is defined as the ratio of the total area of all grains within a reference area to the total area enclosed by the reference area boundary (Ersoy & Waller, 1995). Using five random fields of view per thin section, this property was measured for all the samples. Also, texture coefficient (TC), as suggested by Howarth and Rowlands (1986), were calculated for all the samples (Table 2).

On the other hand, physical properties such as the dry density (γd), the saturated density (γsat), the porosity (n), and the specific gravity (Gs), as well as the tensile strength tests were performed in accordance to ISRM (1981). The physical properties of the sandstones are shown in Table 3. The tensile strengths of the rock samples were determined using Brazilian tensile strength tests (BTS) under dry conditions.

## Results and Discussion

### *Mineral compositions*

In general, the examined sandstones are mainly composed of lithic fragments, quartz, chert, opaque minerals, feldspar, and mica. The relative mineral composition for all sandstones is summarized in Table 1. Lithic fragments are often carbonaceous, volcanic, metamorphic, as well as muddy.

However, the most abundant of rock fragments in the sandstones is the carbonaceous rock fragment (CRF). The average total CRF content was 55.93% (Table 1). In these samples, Quartz, Chert, and opaque minerals vary from 2 to 20%, 0 to 10%, and 1 to 10%, respectively.

Modal analyses reveal that the feldspar content is generally between 0 to 9%. Feldspar is both K-feldspar and plagioclase. The mica content is of little or no importance (Table 1).

All except sample No. 8 are classified as calclitharenite according to the classification provided by Folk (1974). Accordingly, sample No. 8 is a volcarenite. Moreover, all except samples No. 8, 9, 10, 11 and 12 contain variable amounts of cement, the mean content being 7.55% (Table 1). The cement type for these sandstones except sample No. 1 (gypsum) is calcite.

*Textural characteristics*

The studied sandstones have a fairly wide spectrum of grain sizes. The grain size distributions are shown in Table 2.

The medium grain size in sandstone samples is 0.47 mm in diameter. The finest grain size is observed on sample No. 17 while the largest is on sample No. 19 (Table 2).

Table 2. Measured texture data for twenty-nine sandstone specimens

| Sample No. | MGS (mm) | AR | FF | GAR | PD(%) | PP(%) | GC(%) | Type of contact (%) | | | | | TC |
|---|---|---|---|---|---|---|---|---|---|---|---|---|---|
| | | | | | | | | FC | TaC | LC | C-C | Su | |
| 1 | 0.57 | 1.78 | 0.675 | 0.638 | 85.30 | 61.60 | 74.82 | 33 | 8 | 31 | 27 | 1 | 2.42 |
| 2 | 0.74 | 1.79 | 0.601 | 0.844 | 98.05 | 79.46 | 89.21 | 2 | 23 | 20 | 22 | 33 | 2.11 |
| 3 | 0.32 | 1.77 | 0.593 | 0.860 | 96.73 | 73.85 | 95.14 | 6 | 11 | 44 | 27 | 13 | 3.12 |
| 4 | 0.44 | 1.88 | 0.63 | 0.900 | 98.29 | 79.32 | 95.56 | 2 | 13 | 28 | 22 | 35 | 2.43 |
| 5 | 0.43 | 1.49 | 0.569 | 0.834 | 94.80 | 71.43 | 94.28 | 7 | 24 | 40 | 19 | 10 | 1.55 |
| 6 | 0.48 | 1.98 | 0.632 | 0.897 | 92.37 | 59.65 | 84.36 | 14 | 35 | 27 | 13 | 11 | 1.66 |
| 7 | 0.42 | 1.8 | 0.665 | 0.728 | 81.40 | 54.53 | 81.44 | 31 | 22 | 37 | 9 | 1 | 2.79 |
| 8 | 0.53 | 1.85 | 0.686 | 0.805 | 82.18 | 53.69 | 66.76 | 20 | 41 | 33 | 5 | 1 | 1.93 |
| 9 | 0.44 | 2.02 | 0.600 | 0.847 | 84.80 | 61.56 | 76.53 | 9 | 58 | 24 | 5 | 4 | 1.63 |
| 10 | 0.69 | 1.83 | 0.633 | 0.813 | 82.60 | 53.76 | 72.66 | 19 | 46 | 31 | 3 | 1 | 2.21 |
| 11 | 0.41 | 1.91 | 0.605 | 0.788 | 80.71 | 53.92 | 81.89 | 51 | 36 | 10 | 2 | 1 | 1.93 |
| 12 | 0.46 | 0.89 | 0.588 | 0.783 | 82.70 | 53.04 | 83.78 | 55 | 24 | 16 | 3 | 2 | 3.62 |
| 13 | 0.32 | 1.73 | 0.632 | 0.806 | 96.76 | 72.44 | 92.94 | 6 | 19 | 32 | 23 | 19 | 2.52 |
| 14 | 0.43 | 1.66 | 0.594 | 0.861 | 90.55 | 68.75 | 90.08 | 15 | 33 | 28 | 13 | 11 | 3.18 |
| 15 | 0.39 | 2.26 | 0.630 | 0.865 | 96.31 | 76.09 | 87.98 | 9 | 23 | 25 | 21 | 22 | 2.89 |
| 16 | 0.56 | 1.83 | 0.603 | 0.913 | 93.45 | 77.04 | 85.65 | 7 | 23 | 22 | 17 | 31 | 2.99 |
| 17 | 0.18 | 1.73 | 0.637 | 0.880 | 90.92 | 73.21 | 84.55 | 9 | 26 | 21 | 14 | 30 | 2.58 |
| 18 | 0.62 | 1.57 | 0.604 | 0.862 | 87.50 | 65.81 | 82.83 | 22 | 32 | 15 | 12 | 19 | 2.63 |
| 19 | 0.86 | 1.7 | 0.648 | 0.859 | 87.56 | 53.67 | 77.85 | 26 | 37 | 15 | 13 | 9 | 2.71 |
| 20 | 0.61 | 1.75 | 0.613 | 0.847 | 96.14 | 78.57 | 95.66 | 1 | 27 | 13 | 6 | 53 | 2.56 |
| 21 | 0.45 | 1.62 | 0.64 | 0.913 | 93.14 | 73.59 | 88.92 | 1 | 36 | 12 | 8 | 43 | 2.36 |
| 22 | 0.49 | 1.73 | 0.64 | 0.879 | 94.16 | 76.36 | 89.81 | 1 | 34 | 6 | 5 | 54 | 3.02 |
| 23 | 0.47 | 1.75 | 0.565 | 0.844 | 92.97 | 71.43 | 85.39 | 8 | 40 | 12 | 13 | 27 | 2.84 |
| 24 | 0.31 | 1.67 | 0.636 | 0.869 | 94.76 | 78.01 | 92.06 | 1 | 31 | 10 | 7 | 52 | 2.49 |
| 25 | 0.26 | 1.65 | 0.582 | 0.869 | 92.18 | 73.83 | 87.22 | 1 | 34 | 11 | 8 | 47 | 2.42 |
| 26 | 0.44 | 1.75 | 0.823 | 0.822 | 92.98 | 74.85 | 88.22 | 1 | 26 | 15 | 10 | 49 | 2.23 |
| 27 | 0.6 | 2.01 | 0.583 | 0.837 | 92.24 | 70.37 | 87.92 | 1 | 22 | 23 | 9 | 46 | 1.64 |
| 28 | 0.32 | 1.93 | 0.558 | 0.837 | 88.78 | 65.26 | 82.84 | 19 | 26 | 15 | 7 | 30 | 2.00 |
| 29 | 0.53 | 1.87 | 0.615 | 0.837 | 90.12 | 68.33 | 84.33 | 3 | 22 | 19 | 6 | 50 | 2.24 |
| Mean | 0.47 | 1.76 | 0.629 | 0.840 | 90.71 | 67.5 | 82.78 | 13.1 | 28.69 | 21.9 | 12.03 | 24.31 | 2.44 |
| SD | 0.15 | 0.23 | 0.05 | 0.060 | 5.34 | 10.07 | 17.13 | 14.5 | 10.57 | 9.85 | 7.36 | 18.89 | 0.51 |

GS: Medium grain size, AR: Aspect ratio, FF: Form factor, GAR: Grain area ratio, PD: Packing density, PP: Packing proximity, GC: Grain contact, FC: Floating contact, TaC: Tangential contact, LC: Long contact, C-C: Concavo-convex contact, Su: Sutured contact, TC: Texture coefficient

Table 3. Physical properties and tensile strengths of the rocks used in the experiments

| Sample No. | Porosity (%) | Specific gravity (Gs) | Dry unit weight (kN/m$^3$) | Saturated unit weight (kN/m$^3$) | Dry tensile strength (MPa) |
|---|---|---|---|---|---|
| 1 | 18.35 | 26.68 | 21.78 | 23.54 | 3.85 |
| 2 | 5.74 | 24.33 | 22.86 | 23.45 | 8.64 |
| 3 | 12.51 | 24.62 | 21.58 | 22.76 | 4.31 |
| 4 | 5.05 | 24.92 | 23.64 | 24.13 | 10.18 |
| 5 | 14.05 | 24.13 | 20.70 | 22.17 | 2.45 |
| 6 | 14.94 | 23.94 | 20.40 | 21.88 | 2.69 |
| 7 | 23.66 | 23.35 | 17.85 | 20.21 | 0.72 |
| 8 | 23.17 | 23.74 | 18.25 | 20.50 | 0.61 |
| 9 | 19.82 | 23.45 | 18.83 | 20.70 | 1.54 |
| 10 | 24.89 | 23.64 | 17.76 | 20.21 | 0.49 |
| 11 | 24.22 | 23.25 | 17.66 | 20.01 | 0.22 |
| 12 | 25.27 | 22.76 | 16.97 | 19.42 | 0.19 |
| 13 | 6.82 | 25.41 | 23.64 | 24.33 | 9.23 |
| 14 | 10.43 | 25.41 | 22.76 | 23.84 | 4.56 |
| 15 | 5.39 | 24.82 | 23.44 | 23.94 | 10.13 |
| 16 | 4.19 | 25.11 | 24.03 | 24.43 | 8.60 |
| 17 | 5.89 | 25.90 | 24.33 | 24.92 | 9.62 |
| 18 | 17.67 | 23.35 | 19.23 | 20.99 | 2.4 |
| 19 | 17.59 | 23.74 | 19.52 | 21.29 | 2.00 |
| 20 | 4.29 | 24.92 | 23.84 | 24.23 | 10.49 |
| 21 | 4.24 | 25.21 | 24.13 | 24.62 | 9.60 |
| 22 | 4.53 | 25.51 | 24.33 | 24.82 | 9.70 |
| 23 | 5.52 | 24.62 | 22.76 | 23.54 | 5.45 |
| 24 | 4.56 | 25.8 | 24.62 | 25.11 | 8.59 |
| 25 | 7.65 | 25.6 | 23.64 | 24.33 | 8.00 |
| 26 | 4.47 | 25.51 | 24.33 | 24.82 | 13.23 |
| 27 | 4.25 | 25.7 | 24.62 | 25.01 | 9.82 |
| 28 | 8.83 | 25.7 | 23.45 | 24.33 | 5.76 |
| 29 | 5.37 | 25.6 | 24.23 | 24.72 | 8.07 |
| Mean | 11.49 | 24.71 | 21.90 | 23.04 | 5.90 |
| SD | 7.66 | 1.00 | 2.55 | 1.84 | 3.95 |

In these sandstones, the mean values for aspect ratio, form factor, and grain area ratio are 1.76, 0.629, and 0.840, respectively. Packing density and packing proximity represent the internal relation and arrangement of grains' rock. For the studied sandstones, packing proximity ranges from 45.10 to 79.46% and packing density ranges from 80.60 to 98.29%. The lower values of packing proximity indicate that grains are not necessarily tightly interlocked. This situation can be attributed to their high porosity percentage. Table 2 shows that the majority of grain contacts are of the tangential and sutured types, the average values being 28.69 and 24.31%, respectively. The concave-convex type is the least common.

On the other hand, sutured contacts are representative of grains which have undergone high overburden pressures, whilst long, tangential, and concave-convex contacts demonstrate intermediate stages of digenesis (Bell & Culshaw, 1978). Therefore, the examined sandstones probably represent the intermediate to high stages. The highest grain contact percentage is found on sample No. 20 while the lowest one is found on sample No. 8. Also, there is variation in the texture coefficients of all the sandstones studied from 1.55 to 3.62.

*Physical properties and tensile strength*

The values of physical properties and tensile strength are presented in Table 3. The dry unit weight varies from 16.97 to 24.62 kN/m$^3$ and the saturated unit weight ranges from 19.42 to 25.01 kN/m$^3$. Porosity varies between 4.24 and 25.27%. The tensile strength of the sandstones ranges from a minimum of 0.19 MPa for sample No.12 to a maximum of 13.23 MPa for sample No. 26, with a mean of 5.9 MPa and a standard deviation of 3.95 MPa.

*Development of models*

*Regression models*

In this study, regression analyses are conducted to

predict the tensile strength ($\sigma_t$) of the sandstones in terms of mineral and textural features. For this reason, mainly two statistical models, namely, simple linear regression model and multiple regression model, were developed. Initially, simple regression analyses were conducted to identify the type of relationship between the two parameters. During the simple regression analyses, linear and non-linear functions were employed. Also, the equations of the best-fit line, the determination coefficient ($R^2$) and the 95% confidence limits were computed for each regression. All statistical analyses including F- and T-tests were performed using IBM SPSS Statistics 21 software (Tables 4 and 5). The results of simple regression analyses are summarized in Table 4.

As it is evident from Table 4, the regressions presented a strong correlation among tensile strength, PD, PP, floating contact, and sutured contact with the determination coefficient ($R^2$) between 0.725 and 0.803. However, the correlations of $\sigma_t$ with GC, concave-convex contact, and cement percentage had moderate correlation ($R^2$=0.225- 0.501). Other textural coefficients had low correlation with tensile strength. On the basis of the results, the petrographical parameters selected in the development of the multiple regression models include the seven recent parameters.

In the second stage, multiple regression analysis is used to derive an equation that can be used to predict values of a dependent variable from several independent variables. Seven of the whole samples in the dataset are used as the validation or control dataset. Accordingly, stepwise multiple regressions were carried out to correlate the measured tensile strength to petrographical properties (Table 5).

As can be seen in Table 5, the highest coefficient of determination ($R^2$) values was achieved when three petroghaphical characteristics of the sandstones, namely, sutured contact, packing density, and cement percentage were used as the input parameters. Consequently, Equation (3) which yielded the highest $R^2$- and F-value as well as T-ratio, is proposed to predict the tensile strength of the sandstones (model No. 5).

Table 4. Summary of simple regression analyses between petrographical characteristics and tensile strength of the Aghajari sandstones

| Predictor | Predicted equation | $R^2$ | T-ratio | F-value | Probability |
|---|---|---|---|---|---|
| Aspect ratio (AR) | $\sigma_t=2.866AR^{0.76}$ | 0.132 | 2.022 | 4.089 | 0.053 |
| Medium grain size (MGS) | $\sigma_t=3.687-2.792$Log MGS | 0.053 | -1.228 | 1.508 | 0.22 |
| Grain area ratio (GAR) | $\sigma_t=9.883e^{0.001GAR}$ | 0.206 | 2.649 | 7.019 | 0.013 |
| Form factor (FF) | $\sigma_t=18.361$FF$-5.547$ | 0.054 | 1.236 | 1.529 | 0.227 |
| Packing density (PD) | $\sigma_t=5.36\times10^{-34}PD^{17.296}$ | 0.725 | 8.434 | 71.134 | 0.000 |
| Packing proximity (PP) | $\sigma_t=1.811\times10^{-14}PP^{7.829}$ | 0.803 | 10.490 | 110.044 | 0.000 |
| Grain contact (GC) | $\sigma_t=0.034e^{0.231GC}$ | 0.225 | 2.801 | 7.847 | 0.009 |
| Floating contact | $\sigma_t=9.59e^{-0.071\text{Floating contact}}$ | 0.725 | -8.436 | 71.17 | 0.000 |
| Tangential contact | $\sigma_t=9.781-0.135$Tangential contact | 0.131 | -2.016 | 4.064 | 0.054 |
| Long contact | $\sigma_t=8.794-0.132$Long contact | 0.109 | -1.813 | 3.288 | 0.81 |
| Concave-convex contact | $\sigma_t=0.374$ Concave-convex contact$^{1.012}$ | 0.331 | 3.654 | 13.35 | 0.001 |
| Sutured contact | $\sigma_t=0.549$Sutured contact$^{0.748}$ | 0.774 | 9.621 | 92.562 | 0.000 |
| Texture coefficient (TC) | $\sigma_t=3.939+2.259$Log TC | 0.015 | 0.651 | 0.423 | 0.521 |
| Litic | $\sigma t=85.22$ Litic$^{-0.045}$ | 0.114 | -1.864 | 3.475 | 0.073 |
| Quartz (Q) | $\sigma_t=4.874Q^{-0.118}$ | 0.004 | -0.316 | 0.1 | 0.755 |
| Chert (CH) | $\sigma_t=2.955CH^{0.058}$ | 0.019 | 0.716 | 0.513 | 0.48 |
| Feldespars (F) | $\sigma_t=7.367-0.582$Fel | 0.1 | -1.734 | 3.007 | 0.094 |
| Opaque minerals (Opq) | $\sigma_t=12.703e^{-0.257Opq}$ | 0.201 | -2.607 | 6.799 | 0.015 |
| Cement (Cm) | $\sigma_t=2.766+0.417$Cm | 0.501 | 5.201 | 27.055 | 0.000 |

Table 5. Stepwise multiple regression analyses to estimate tensile strength from petrographical characteristics

| Dependent variable | Model No. | Predictor | coefficient | $R^2$ | T-ratio | F-value | Probability |
|---|---|---|---|---|---|---|---|
| Dry $\sigma_t$ | 1 | Constant | -8.582 | 0.877 | -1.273 | 14.219 | 0.224 |
| | | Packing densiry | 0.268 | | 0.964 | | 0.352 |
| | | Grain contact | -0.008 | | -0.353 | | 0.729 |
| | | Packing proximity | -0.130 | | -0.537 | | 0.600 |
| | | Float contact | 0.033 | | 0.617 | | 0.547 |
| | | Sutured contact | 0.127 | | 2.486 | | 0.026 |
| | | Concave-convex contact | 0.093 | | 0.936 | | 0.365 |
| | | Cement | 0.128 | | 1.765 | | 0.099 |
| | 2 | Constant | -8.568 | 0.876 | -1.310 | 17.595 | 0.210 |
| | | Packing densiry | 0.257 | | .958 | | 0.353 |
| | | Packing proximity | -0.128 | | -.547 | | 0.592 |
| | | Float contact | 0.033 | | 0.635 | | 0.535 |
| | | Sutured contact | 0.128 | | 2.568 | | 0.021 |
| | | Concave-convex contact | 0.093 | | 0.966 | | 0.349 |
| | | Cement | .127 | | 1.808 | | 0.091 |
| | 3 | Constant | -7.577 | 0.873 | -1.232 | 22.017 | 0.236 |
| | | Packing densiry | 0.122 | | 1.165 | | 0.261 |
| | | Float contact | 0.023 | | 0.482 | | 0.637 |
| | | Sutured contact | 0.119 | | 2.577 | | 0.020 |
| | | Concave-convex contact | 0.076 | | 0.853 | | 0.406 |
| | | Cement | 0.129 | | 1.885 | | 0.078 |
| | 4 | Constant | -5.816 | 0.871 | -1.204 | 28.763 | 0.245 |
| | | Packing densiry | 0.103 | | 1.086 | | 0.293 |
| | | Sutured contact | 0.115 | | 2.591 | | 0.019 |
| | | Concave-convex contact | 0.073 | | 0.835 | | 0.415 |
| | | Cement | 0.130 | | 1.942 | | 0.069 |
| | 5 | Constant | -8.540 | 0.866 | -2.419 | 38.772 | 0.026 |
| | | Packing densiry | 0.164 | | 2.768 | | 0.013 |
| | | Sutured contact | 0.086 | | 3.201 | | 0.005 |
| | | Cement | 0.147 | | 2.320 | | 0.032 |

$\sigma_t$=0.164 Packing density +0.086 Sutured contact + 0.147 Cement -8.540 (3)

In addition, predicted tensile strengths were compared to actual measured values for testing samples. For this purpose, the measured variables were substituted in this equation to predict tensile strength (Fig. 3). As it is evident, the error of data from the 1:1 line is very low ($R^2$=0.946). Thus, the prediction equations can be used to obtain rough estimates of tensile strength.

*Artificial neural network model*

Artificial neural networks (ANN) are essentially connectionist systems, in which various nodes, called neurons, are linked to one another. A neuron receives one or more input signals and, depending on the processing function involved, provides an output signal. This output is transferred to other neurons with different intensities, based on the weights specified (Kasabov, 1996).

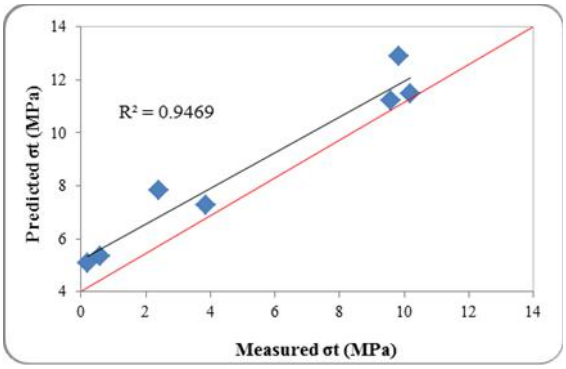


Figure 3. Comparison of predicted and measured tensile strengths of testing samples for estimating model

A feed forward network involves an order of layers, each layer including several neurons. The output of the neurons of a layer is input to the neurons of the next layer. The first and last layer of ANN is called the input and the output layers, respectively. The input layer does not perform any computations, but only serves to feed the input data to the hidden layer which is between the input and output layers. The presence of hidden layers provides complexity for the network architecture and this complexity is employed for modeling nonlinear relationships (Kasabov, 1996).

Depending on the presence or lack of feedback in the architecture of a neural network, there are two separate types of networks, namely with feedback architecture and with feed-forward architecture, respectively. In feed-forward architecture, there is no returning connection from output neurons to the input neurons. A network with feed-forward architecture has been employed in the present study.

Different algorithms can be used to train a network. In general, the training algorithms can be divided into two types: supervised and unsupervised. In supervised learning, input data are related to a specified output, i.e., the learning process is performed with pairs of data. The unsupervised learning method is used where the output or target values are unspecified (Kamruzzaman *et al.*, 2006). Selection of the best and fastest learning algorithm for solving a problem is very important and difficult. One common algorithm for adjusting the weights is a back-propagation algorithm. This algorithm, which is a sort of supervised learning technique, is employed in this investigation.

A network starts working with a set of initial weights and then gradually modifies the weights in a training cycle until the desired weights are achieved. The desired weights perform the input-output mapping with the least error. The training process contains two passes, namely forward and reverse passes. In a forward pass, the input signals are distributed from the input to the output of the network. In the reverse pass, however, the calculated error signals are taken backward in the network in order to adjust the values of the weights. Calculation of the output is carried out layer by layer and in the forward direction. The output of a layer is the input for the subsequent layer. In the reverse pass, the weights of the output neurons are initially adjusted because the target value of each output neuron is available. Afterward, the weights of the middle layers are changed. Because there is no target value for a middle layer, the errors of previous layers are taken backwards layer by layer in the network. This algorithm is called a back-propagation algorithm. The trained network is then validated with a set of data. If the testing error is greater than the training error, it can be claimed that the network possesses excessive overfitting with the data. For a network with good overfitting, the testing and training errors are reasonably close to each other. Now the trained neural network can be employed for estimating the suitable output for a new set of data. In this study, a two-layer neural network was employed in order to determine the tensile strength of the sandstones. The first layer of the network consisted of 3 neurons with TANSIG activating function. Also, the second layer had one neuron with PURLINE function. Floating contact, sutured contact, concave-convex contact, GC, PD, PP, and cement percentage parameters were used for the input of ANN. These parameters have been chosen based on regression analysis and have an intense effect on the tensile strength. The samples were divided into training and testing data. The twenty-two samples were used for developing the model and the seven samples were used as testing data.

The neural network was trained by changing its inter-layer weights. Equation (4) resulted from finding these weights from the network and the activation function. This expression is simply how the neural network processed the input data to reach the output. A schematic presentation of the neural network is illustrated in Figure 4.

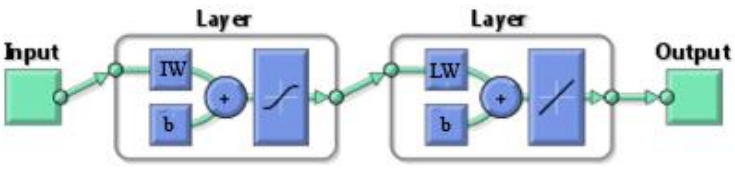


Figure 4. Neural network structure used with details

In figure 4, IW is the first layer weight and b is the layer biases that are specified after network training. Furthermore, LW is the second layer weight. The weight function, therefore, can be applied to the data without having to use and train a neural network again.

Output=(2/(1+exp(-2* (input)/10*IW+b1))-1)*LW+b2 (4)

$$IW = \begin{bmatrix} -0.0276 & -1.6911 & 12.8344 \\ 0.0223 & -16.0843 & -7.9536 \\ -0.0466 & 27.0506 & -21.1119 \\ -0.0265 & 0.2177 & -10.3027 \\ 0.0075 & -16.6411 & -3.9175 \\ 0.0250 & 0.7043 & -0.2782 \\ 0.0223 & 9.8421 & -2.1592 \end{bmatrix}$$

$$b1 = \begin{bmatrix} 1.4599 & -23.1312 & 123.1182 \end{bmatrix}$$

$$LW = \begin{bmatrix} 311.3325 \\ 1.2109 \\ -3.5701 \end{bmatrix}$$

$$b2 = \begin{bmatrix} -244.0805 \end{bmatrix}$$

Performance of the proposed model was evaluated using selected datasets considered for testing the model. The coefficient of determination for measured and predicted tensile strength was computed 0.998 (Fig. 5). Thus, the performance of the ANN models was also compared with other statistical methods (e.g., regression analysis). The study demonstrates that the results of ANN are more precise than the conventional statistical approaches.

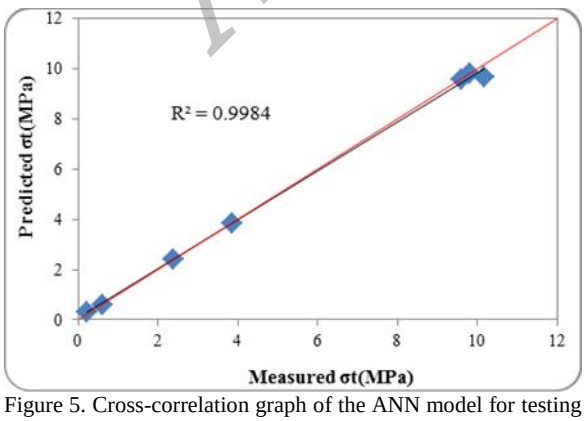


Figure 5. Cross-correlation graph of the ANN model for testing data

## Conclusions

The quantification of textural and mineralogical features as well as tensile strength of sandstones can help to identify the inter-relationship among them. In this study, the relationships among textural features, mineral composition, and tensile strength of twenty-nine selected sandstones from Khouzestan province were estimated by regression analyses and artificial neural network. In general, this study indicates that the influence of textural characteristics appear to be more important than mineralogy for predicting the tensile strength of the sandstones. However, a positive relationship between the cement percentage and the tensile strength of the examined sandstones is found, indicating that the tensile strength decreases with the reduction of cement. Simple regression analyses reveal that the packing proximity, sutured contact, and packing density are the common textural parameters exhibiting significantly positive correlations with tensile strength. However, the tensile strength of the sandstones decreases by increasing the floating contacts.

Model equations were developed as a result of stepwise multiple linear regression analysis and artificial neural network for the prediction of tensile strength from their petrographical features. According to the results of stepwise regression analyses, the key petrographical parameters influencing the tensile strength of the sandstones are determined as packing density, sutured type grain contact, and cement content. Also, among these three parameters, the packing proximity is the most effective parameter. Equation 3 for the prediction of the tensile strength of the sandstones could be used practically. For the artificial neural network, the key petrographical parameters influencing the tensile strength of the sandstones are packing proximity, packing density, sutured contact and floating contact, concave-convex contact, grain contact percentage, and cement content. Thus, the results show the superiority of the neural network over the conventional statistical method. Furthermore, using these equations to predict the tensile strength of the sandstones is easier, faster, and cheaper than conducting tensile strength tests.

**References**

Bell, F.G., Culshaw, M.G., 1978. Petrographic and engineering properties of sandstones from the Sneinton Formation, Nottinghamshire, England. Quarterly Journal of Engineering Geology. 31: 5–21.

Bell, F.G., Lindsay, P., 1999. The petrographical and geomechanical properties of some sandstones from the Newspaper Member of the Natal Group near Durban, South Africa. Engineering Geology. 53: 57–81.

Canakci, H., Pala, M., 2007. Tensile strength of basalt from a neural network. Engineering Geology. 93: 10–18.

Dobereiner, L., De Freitas, M.H., 1986. Geotechnical properties of weak sandstone. Geotechnique. 36 (1): 79–94.

Ersoy, A., Waller, M.D., 1995. Textural characterisation of rocks. Engineering Geology.39: 123 – 136.

Folk, R.L., 1974. Petrology of sedimentary rocks. Hemphill Publication Company, Austin.

Gurocak, Z., Solanki, P., Alemdag, S., Zaman, M.M., 2012. New considerations for empirical estimation of tensile strength of rocks. Engineering Geology. 145-146: 1–8.

Howarth, D.F., Rowlands, J.C., 1986. Development of an index to quantify rock texture for qualitative assessment of intact rock properties. Geotechnical Testing Journal. 9: 169-179.

International society for rock mechanics, 1981. Rock characterization, testing and monitoring, ISRM Suggested Methods. Pergamon Press, Oxford.

James, G.A., Wynd, J.G., 1965. Stratigraphic nomenclature of Iranian Oil Consortium Agreement Area. Bulletin of American Association of Petroleum Geology. 49(12): 2182-2245.

Kahn, J.S., 1956. The analysis and distribution of the properties of packing in sand size sediments. Journal of Geology. 64:385–395.

Kasabov, N.K., 1996. Foundations of Neural Networks, Fuzzy Systems and Knowledge. the MIT press, Cambridge.

Kamruzzaman, J., Begg, R.K., Sarker, R.A., 2006. Neural Networks in Finance and Manufacturing. Idea Group Publishing, Hershey.

Merriam, R., Rieke III, H.H, Kim, Y.C., 1970. Tensile strength related to mineralogy and texture of some granitic rocks. Engineering Geology. 4: 155 – 160.

Nova, A., Zaninetti, R., 1990. An investigation into the tensile behavior of a schistose rock. International Journal of Rock Mechanics and Mining Sciences& Geomechanics Abstracts. 27(1): 231-242.

Ozcelik, Y., Bayram, F., Yasitli, N.E., 2012. Prediction of engineering properties of rock from microscopic data.Arabian Journal of Geosciences.

Prikryl, R., 2001. Some microstructural aspects of strength variation in rocks. International Journal of Rock Mechanics and Mining Sciences. 38: 671– 682.

Tugrul, A., Zarif, I.H., 1999. Correlation of mineralogical and textural characteristics with engineering properties of selected granitic rocks from Turkey. Engineering Geology. 51: 303 – 317.

Tavallali, A., and Vervoort, A., 2010. Failure of layered sandstone under Brazilian test conditions: effect of micro-scale parameters on macro-scale behavior. Rock Mechanics and Rock Engineering. 43(5):641-653.